ISSN 0036-0236, Russian Journal of Inorganic Chemistry, 2022, Vol. 67, No. 4, pp. 497–503. © Pleiades Publishing, Ltd., 2022.
ISSN 0036-0236, Russian Journal of Inorganic Chemistry, 2022. © Pleiades Publishing, Ltd., 2022.

PHYSICOCHEMICAL ANALYSIS OF INORGANIC SYSTEMS

Solid–Liquid Phase Equilibria of the Quaternary System Na^+, Mg^{2+}//Cl^-, $B_4O_7^{2-}$–H_2O at 298.15 K

Chao Gao[a], Xue-min Du[a], Hai-juan Qin[b, *], Ya-fei Guo[a, c], Shi-qiang Wang[a, c, **], and Tian-long Deng[a, c]

[a] *College of Marine and Environmental Sciences, Tianjin University of Science and Technology, Tianjin, 300457 China*
[b] *Research Centre of Modern Analytical Technology, Tianjin University of Science and Technology, Tianjin, 300457 China*
[c] *Key Laboratory of Marine Resource Chemistry and Food Technology (TUST), Ministry of Education, Tianjin, 300457 China*
**e-mail: qinhj@tust.edu.cn*
***e-mail: wangshiqiang@tust.edu.cn*

Received October 11, 2021; revised November 8, 2021; accepted November 10, 2021

Abstract—Solubility data for the quaternary system Na^+, Mg^{2+}//Cl^-, $B_4O_7^{2-}$–H_2O is very important for the separation of magnesium and boron from the salt lake brines in Qaidam Basin. The solubility of the quaternary system Na^+, Mg^{2+}//Cl^-, $B_4O_7^{2-}$–H_2O at $T = 298.15$ K and $p = 0.1$ MPa was investigated experimentally with the method of isothermal dissolution equilibrium, and meanwhile physicochemical properties including density, refractive index and pH value were determined. In the phase diagrams of the quaternary system at 298.15 K, there are two invariant points, five univariant isothermal dissolution curves, and four crystallization regions corresponding to NaCl, $Na_2B_4O_7{\cdot}10H_2O$, $MgCl_2{\cdot}6H_2O$ and $Mg_2B_6O_{11}{\cdot}15H_2O$, respectively. The density, refractive index and pH value of the quaternary system at 298.15 K present a regular variation with the increasing of Mg^{2+} concentration.

Keywords: stable phase equilibrium, phase diagram, borate, inderite
DOI: 10.1134/S0036023622040064

INTRODUCTION

Boron compounds have an important application in glass, ceramics, chemical industry, light industry, nuclear industry and so on because of its own merits: light weight, high strength, heat resistance and other good properties [1]. All aspects of national production and life are inseparable from lithium metal and its compounds, ranging from traditional fields such as glass, metallurgy and ceramics to other front-end fields including aerospace and new energy [2–4]. As the available amounts of solid ores are decreasing, the development of liquid borate mineral resources has become an inevitable tendency in future. Liquid mineral resources are mainly distributed in salt lake brine, seawater, geothermal water, and oil-field water. There are abundant salt lake brine resources in the Qaidam Basin, China with high contents of lithium, magnesium, and boron, which is of great exploitation potential and strategic importance [5, 6].

Due to the change of the coordination number of borate ion B–O, the structure of borate ion in solution is complex and the existing forms are various, such as metaborate (BO_2^-), diborate ($B_2O_4^{2-}$), triborate ($B_3O_5^-$), and polytetraborate ($B_4O_7^{2-}$, $B_6O_{10}^{2-}$) [7]. The existing form of boron depends on its concentration and external conditions, such as coexisting ion species, concentration, pH value, and temperature [8]. The study of the multi-temperature phase diagram is great significance to the development of salt lake brine resources. Therefore, the multi-temperature phase diagram of subsystem containing borate has been studied and reported, such as the ternary system (Na^+, Mg^{2+}//$B_4O_7^{2-}$–H_2O) [9], (Li^+, Mg^{2+}//$B_4O_7^{2-}$–H_2O, Na^+, Mg^{2+}//$B_4O_7^{2-}$–H_2O) [10], (Mg^{2+}//Cl^-, $B_4O_7^{2-}$–H_2O, Mg^{2+}//Cl^-, $B_6O_{11}^{2-}$–H_2O) [11, 12] and (K^+//Cl^-, $B_4O_7^{2-}$–H_2O, K^+//SO_4^{2-}, $B_4O_7^{2-}$–H_2O) [13], the quaternary system (K^+//Cl^-, SO_4^{2-}, $B_4O_7^{2-}$–H_2O) [14], (Li^+, Na^+, Mg^{2+}//$B_4O_7^{2-}$–H_2O) [15–17], (Mg^{2+}//Cl^-, SO_4^{2-}, $B_4O_7^{2-}$–H_2O) [18] and (Na^+, K^+, Mg^{2+}// $B_4O_7^{2-}$–H_2O) [19], the quinary system (Na^+, K^+, Mg^{2+}//SO_4^{2-}, $B_4O_7^{2-}$–H_2O) [20], and the complex system (Li^+, K^+, Rb^+, Mg^{2+}//SO_4^{2-}, $B_4O_7^{2-}$–H_2O) [21]. In order to better separate and purify the sodium, magnesium and borate containing resource from salt-lake brine, the isothermal solubilities and the corresponding solution physicochemical properties including

density, refractive index and pH value for the quaternary system Na^+, $Mg^{2+}//Cl^-$, $B_4O_7^{2-}-H_2O$ at T = 298.15 K and p = 0.1 MPa were presented in this paper.

EXPERIMENTAL

Apparatus and reagents. A magnetic stirring thermostatic water bath (HXC-500-8A, Beijing Fortunejoy Sci. Technol. Co., Ltd.) was used to control the temperature with a precision of 0.01 K. For determining the densities (ρ), a digital densimeter (DMA 4500, Anton Paar Co., Ltd.) that can automatically control the sample cell temperature within 0.01 K was applied with a precision of ±0.15 mg cm^{-3}. In order to measure the refractive index (n_D), an Abbe refractometer (Abbemat 550, Anton Paar Co., Ltd.) with a precision of ±0.0001 was used. The pH value was determined by a high precision PHSJ-5 pH meter (Shanghai Precision Scientific Instruments Co. Ltd., China) with an accuracy of ±0.01. Solid phase was identified by the X-ray powder diffractometer (MSAL XD-3, Beijing Purk Instrument Co., Ltd.).

The chemicals of analytical grade were obtained from the Sinopharm Chemical Reagent Co., Ltd: NaCl (0.995 in mass fraction), $MgCl_2{\cdot}6H_2O$ (0.992 in mass fraction), $Na_2B_4O_7{\cdot}10H_2O$ (0.992 in mass fraction), and were recrystallized with doubly deionized water (DDW) before use. The hungtsaoite ($MgB_4O_7{\cdot}9H_2O$, 0.99 in mass fraction) were synthesized in our lab [22]. Doubly deionized water (DDW) with conductivity less than 1 × 10^{-4} S m^{-1} was used to prepare the series of the artificial synthesized brines and chemical analysis.

Method. The equilibrium experiment in this work was conducted by the method of isothermal dissolution equilibrium [23, 24]. In briefly, the series of artificial synthesized complexes are sealed in hard polyethylene bottles and placed in the magnetic stirring thermostatic bath (HXC-500-8A). The temperature of the bath was checked with a separate thermometer, and the standard deviation of the temperature for 1 day was less than 0.1 K. In order to accelerate the establishment of equilibrium states, the magnetic stirring thermostatic bath was set 150 rpm stirring speed. At regular intervals, the magnetic stirring was paused for 4 h to probe for chemical analysis, and when the composition of the sample became constant, it indicated that the equilibrium had been achieved. It took about 10 days to reach equilibrium for this system. And then, the corresponding solution physicochemical properties including ρ, pH, and n_D were determined, samples of the liquid phase were taken for chemical analysis. In addition, the solid phase minerals were identified with the X-ray powder diffraction.

The concentration of Cl^- in liquid phase was analyzed by titration with $AgNO_3$ standard solution in the presence of potassium chromate indicator. The concentration of boron in liquid phase was analyzed by the gravimetric methods of mannitol with sodium hydroxide standard solution in the presence of double indicator of methyl red and phenolphthalein. The Mg^{2+} ion concentration was determined with modified EDTA complexometric titration method in the presence of Eriochrome Black-T as an indicator, and the uncertainty of the analytical results is less than ±0.003 in mass fraction. The Na^+ ion concentration was evaluated according to ion balance.

RESULTS AND DISCUSSION

Phase Diagram of the Quaternary System Na^+, $Mg^{2+}//Cl^-$, $B_4O_7^{2-}-H_2O$

The experimental data on the solubilites of the quaternary system Na^+, $Mg^{2+}//Cl^-$, $B_4O_7^{2-}-H_2O$ at 298.15 K were determined and are presented in Table 1. The composition of the liquid phase in the quaternary system was expressed in mass fraction (w_b) and Jänecke index [J_b/(mol/100 mol)], with $J(2Na^+)$ + $J(Mg^{2+})$ = 100. The calculating formula for J_b is

$$J_b = \frac{n_b}{n(2Na^+) + n(Mg^{2+})} \times 100.$$

The calculating formula for water concentration is

$$J(H_2O) = \frac{w_{(H_2O)}}{18.0153[n(2Na^+) + n(Mg^{2+})]} \times 100.$$

The J refers to the calculated Jänecke indices of different substances, which reflects the percentage of various ions or water relative to the total equivalent valence moles of cations (anions) based on the principle of equivalent mole valence in the reciprocal quaternary system.

On the basis of the experimental data in Table 1, the phase diagrams of the quaternary system at 298.15 K were plotted, as shown in Figs. 1 and 2. In Fig. 1, the dry-salt phase diagram consists of four crystallization zones corresponding to sodium chloride (NaCl), bischofite ($MgCl_2{\cdot}6H_2O$), borax ($Na_2B_4O_7{\cdot}10H_2O$) and inderite ($Mg_2B_6O_{11}{\cdot}15H_2O$). Hungchaoite ($MgB_4O_7{\cdot}9H_2O$), an incongruently dissolved solid, represents a metastable phase, which easily convert to $Mg_2B_6O_{11}{\cdot}15H_2O$ in this system. As can be seen in Fig. 1, because of the transformation of equilibrium solid phase from hungchaoite ($MgB_4O_7{\cdot}9H_2O$) to inderite ($Mg_2B_6O_{11}{\cdot}15H_2O$) with low solubility, the crystallization field of $Mg_2B_6O_{11}{\cdot}15H_2O$ is the largest, while the $MgCl_2{\cdot}6H_2O$ is the smallest. The size of the mineral crystallization zone is in the order $Mg_2B_6O_{11}{\cdot}15H_2O$ > NaCl > $Na_2B_4O_7{\cdot}10H_2O$ > $MgCl_2{\cdot}6H_2O$. With increasing of the temperature, the solubilities of different salts have changed in the system, which may be shown on the changes of the crystallization fields. To explaining the causes of the formation of the salt and

Table 1. Solubility, density, refractive index and pH of the quaternary system (Na^+, Mg^{2+}//Cl^-, $B_4O_7^{2-}$–H_2O) at 298.15 K

No.	Composition in the solution $100w_b$					Janecke index J_b, mol/100 mol			Density ρ, g cm^{-3}	n_D	pH	Solid phase
	$w(Na^+)$	$w(Mg^{2+})$	$w(Cl^-)$	$w(B_4O_7^{2-})$	$w(H_2O)$	$J(Mg^{2+})$	$J(B_4O_7^{2-})$	$J(H_2O)$				
1, E_1	10.39	0.00	15.75	0.6	73.26	0.00	1.71	1799.63	1.2034	1.3803	8.49	Ha + Borax
2	10.39	0.03	15.82	0.63	73.13	0.54	1.79	1786.59	1.2028	1.3802	8.47	Ha + Borax
3	10.29	0.05	15.72	0.64	73.30	0.91	1.83	1801.47	1.1949	1.3785	8.44	Ha + Borax
4, F_1	10.34	0.05	15.80	0.64	73.17	0.91	1.82	1789.73	1.20000	1.3800	8.44	Ha + Borax + Ind
5	9.65	0.04	14.75	0.55	75.01	0.78	1.67	1968.53	1.1708	1.3732	8.6	Borax + Ind
6	5.86	0.04	8.88	0.60	84.62	1.27	2.99	3638.56	1.1106	1.3594	8.79	Borax + Ind
7	2.36	0.02	3.09	1.32	93.21	1.58	16.30	9920.75	1.0466	1.3440	8.57	Borax + Ind
8	2.08	0.02	2.43	1.84	93.63	1.79	25.73	11284.11	1.0389	1.3420	8.68	Borax + Ind
9	1.25	0.01	1.21	1.63	95.90	1.49	38.05	19288.49	1.0288	1.3394	9.18	Borax + Ind
10	0.91	0.01	0.46	2.12	96.50	2.04	67.60	26512.75	1.0252	1.3384	9.41	Borax + Ind
11	0.90	0.01	0.31	2.43	96.35	2.06	78.32	26761.56	1.0270	1.3386	–	Borax + Ind
12	0.89	0.01	0.15	2.73	96.22	2.08	88.96	27017.37	1.0274	1.3387	9.38	Borax + Ind
13, E_2	0.67	0.01	0.01	2.31	97.00	2.75	99.31	35936.86	1.0259	1.3389	9.52	Borax + Ind
14	9.80	0.42	15.79	1.21	72.78	7.50	3.38	1753.40	1.2063	1.3819	7.23	Ha + Ind
15	9.44	0.74	15.93	1.72	72.17	12.91	4.70	1699.22	1.2023	1.3815	7.03	Ha + Ind
16	8.48	1.19	15.78	1.68	72.87	20.98	4.64	1733.07	1.2083	1.3841	6.3	Ha + Ind
17	6.89	2.14	16.10	1.69	73.18	37.01	4.58	1707.59	1.2133	1.3870	5.98	Ha + Ind
18	6.00	2.69	16.52	1.27	73.52	45.89	3.39	1692.16	1.2133	1.3883	6.06	Ha + Ind
19	4.86	3.47	17.16	1.01	73.50	57.46	2.62	1642.09	1.2162	1.3909	5.91	Ha + Ind
20	3.99	4.1	17.55	1.23	73.13	66.03	3.10	1588.93	1.2240	1.3939	6.26	Ha + Ind
21	3.09	4.69	18.01	0.96	73.25	74.17	2.38	1562.86	1.2304	1.3974	–	Ha + Ind
22	2.12	5.37	18.42	1.13	72.96	82.73	2.73	1516.55	1.2370	1.3997	6.06	Ha + Ind
23	1.40	6.19	19.78	0.95	71.68	89.32	2.15	1395.39	1.2509	1.4020	5.57	Ha + Ind
24	0.97	6.38	19.63	1.04	71.98	92.56	2.36	1408.82	1.2610	1.4056	5.61	Ha + Ind
25	0.70	6.65	20.09	0.86	71.70	94.73	1.92	1378.02	1.2912	1.4176	4.74	Ha + Ind
26	0.57	6.82	20.39	0.85	71.37	95.77	1.87	1352.17	1.2946	1.4176	4.75	Ha + Ind
27, F_2	0.27	7.79	22.78	0.79	68.37	98.20	1.56	1162.76	1.3221	1.4273	4.48	Ha + Ind + Bis
28	0.09	8.66	25.04	0.80	65.41	99.45	1.44	1013.49	1.2927	1.4186	4.97	Ind + Bis
29, E_4	0.00	7.99	22.83	1.06	68.12	100.00	2.08	1150.30	1.2871	1.4172	5.35	Ind + Bis
30, E_3	0.07	9.11	26.68	0.00	64.14	99.60	0.00	945.96	1.3344	1.4316	6.57	Ha + Bis
31	0.13	9.09	26.50	0.49	63.79	99.25	0.84	939.74	1.3395	1.4322	3.46	Ha + Bis
32	0.26	9.16	26.83	0.65	63.10	98.52	1.09	915.68	1.3309	1.4298	4.32	Ha + Bis

Ind—$Mg_2B_6O_{11}\cdot 15H_2O$, Borax—$Na_2B_4O_7\cdot 10H_2O$, Ha—NaCl, Bis—$MgCl_2\cdot 6H_2O$. –, Not detected.

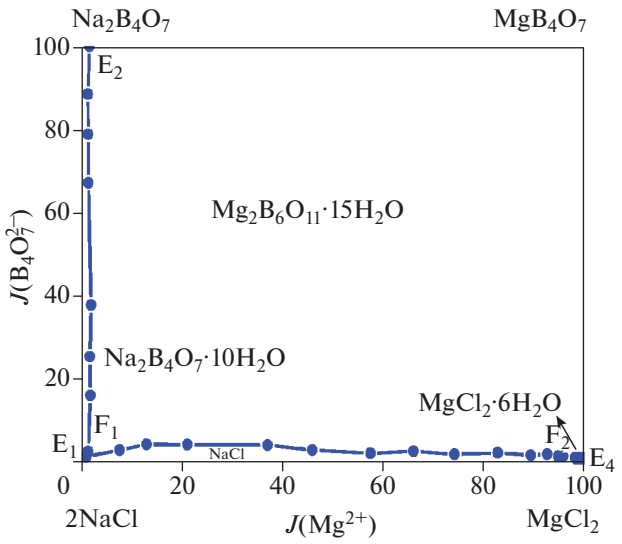

Fig. 1. Dry-salt phase diagram of the quaternary system (Na^+, Mg^{2+}//Cl^-, $B_4O_7^{2-}$–H_2O) at 298.15 K; (•) liquid phase, (–) isotherm curve.

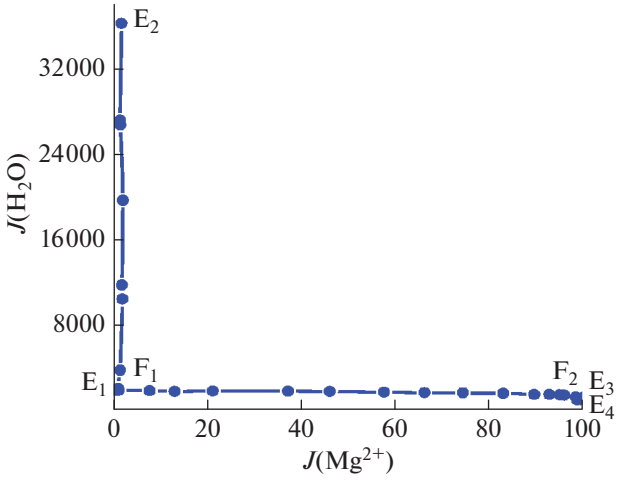

Fig. 2. Water-phase diagram of the quaternary system (Na^+, Mg^{2+}//Cl^-, $B_4O_7^{2-}$–H_2O) at 298.15 K.

the order of crystallization zone in the salt-water system would help choose the best stage for extracting one component or another from the brines in developing technological processes.

There are five univariant curves corresponding to E_1F_1 ($Na_2B_4O_7\cdot10H_2O$ + NaCl), E_2F_1 ($Mg_2B_6O_{11}\cdot15H_2O$ + $Na_2B_4O_7\cdot10H_2O$), F_1F_2 (NaCl + $Mg_2B_6O_{11}\cdot15H_2O$), E_3F_2 ($MgCl_2\cdot6H_2O$ + NaCl) and F_2E_4 ($Mg_2B_6O_{11}\cdot15H_2O$ + $MgCl_2\cdot6H_2O$), indicating the cosaturation of two salts, respectively.

Three invariant points F_1 and F_2 cosaturated with three minerals are marked as follows:

Point F_1 is saturated with salts NaCl + $Na_2B_4O_7\cdot10H_2O$ + $Mg_2B_6O_{11}\cdot15H_2O$. The mass fraction composition of the corresponding liquid phase is $w(Na^+)$ = 10.34%, $w(Mg^{2+})$ = 0.05%, $w(Cl^-)$ = 15.80%, $w(B_4O_7^{2-})$ = 0.64%, and $w(H_2O)$ = 73.17%.

Point F_2 is saturated with salts NaCl + $MgCl_2\cdot6H_2O$ + $Mg_2B_6O_{11}\cdot15H_2O$. The mass fraction composition of the corresponding liquid phase is $w(Na^+)$ = 0.27%, $w(Mg^{2+})$ = 7.79%, $w(Cl^-)$ = 22.78%, $w(B_4O_7^{2-})$ = 0.79%, and $w(H_2O)$ = 68.37%.

In Fig. 2, the ordinate is the Jänecke index of water, and the abscissa is the Jänecke index of magnesium. It can be further found that Jänecke index values of $J(H_2O)$ are changed regularly with the change of $J(Mg^{2+})$, and have singularity changes at the invariant points. As can be seen in Fig. 2, the values of $J(H_2O)$ in the univariant solubility isothermal curve of E_2F_1 are decreased sharply with increasing of $J(Mg^{2+})$ at 298.15 K. On the univariant solubility isothermal curves of F_1F_2, F_2E_3 and F_2E_4, the values of $J(H_2O)$ are gradually decreased with the increase of $J(Mg^{2+})$.

Figure 3 shows the identification results of the solid phase minerals using an X-ray diffractometer. Figure 3a shows the XRD pattern of mineral $Mg_2B_6O_{11}\cdot15H_2O$. Figure 3b shows the XRD pattern of point F_1, which was well matched to the standard diffraction pattern of NaCl, $Na_2B_4O_7\cdot10H_2O$ and $Mg_2B_6O_{11}\cdot15H_2O$ with powder diffraction file (pdf) nos. 02-0818, 12-0258, and 11-0583, respectively.

Solution Physicochemical Properties of the Quaternary System

The solution physicochemical properties including density, refractive index and pH value of the quaternary system Na^+, Mg^{2+}//Cl^-, $B_4O_7^{2-}$–H_2O at 298.15 K were determined and are presented in Table 1, and the diagram of solution density, refractive index and pH value with the concentration of $J(Mg^{2+})$ were plotted in Fig. 4.

In Figs. 4a, 4b, solution density and refractive index have the same tendency. The density values of the equilibrium liquid phase increased gradually with the increasing concentration of $J(Mg^{2+})$ in the solubility isotherm curves of E_2F_1, F_1F_2, and F_2E_3 because of the addition of the other salt, and decreased with the increasing concentration of $J(Mg^{2+})$ in the solubility isotherm curves of E_1F_1 and F_2E_4.

Figure 4c shows the pH value versus composition of $J(Mg^{2+})$ in the solution. The pH values of the equilibrium liquid phase increased gradually with the increasing concentration of $J(Mg^{2+})$ in the solubility isotherm curves of E_1F_1, F_2E_4, and F_2E_3, and

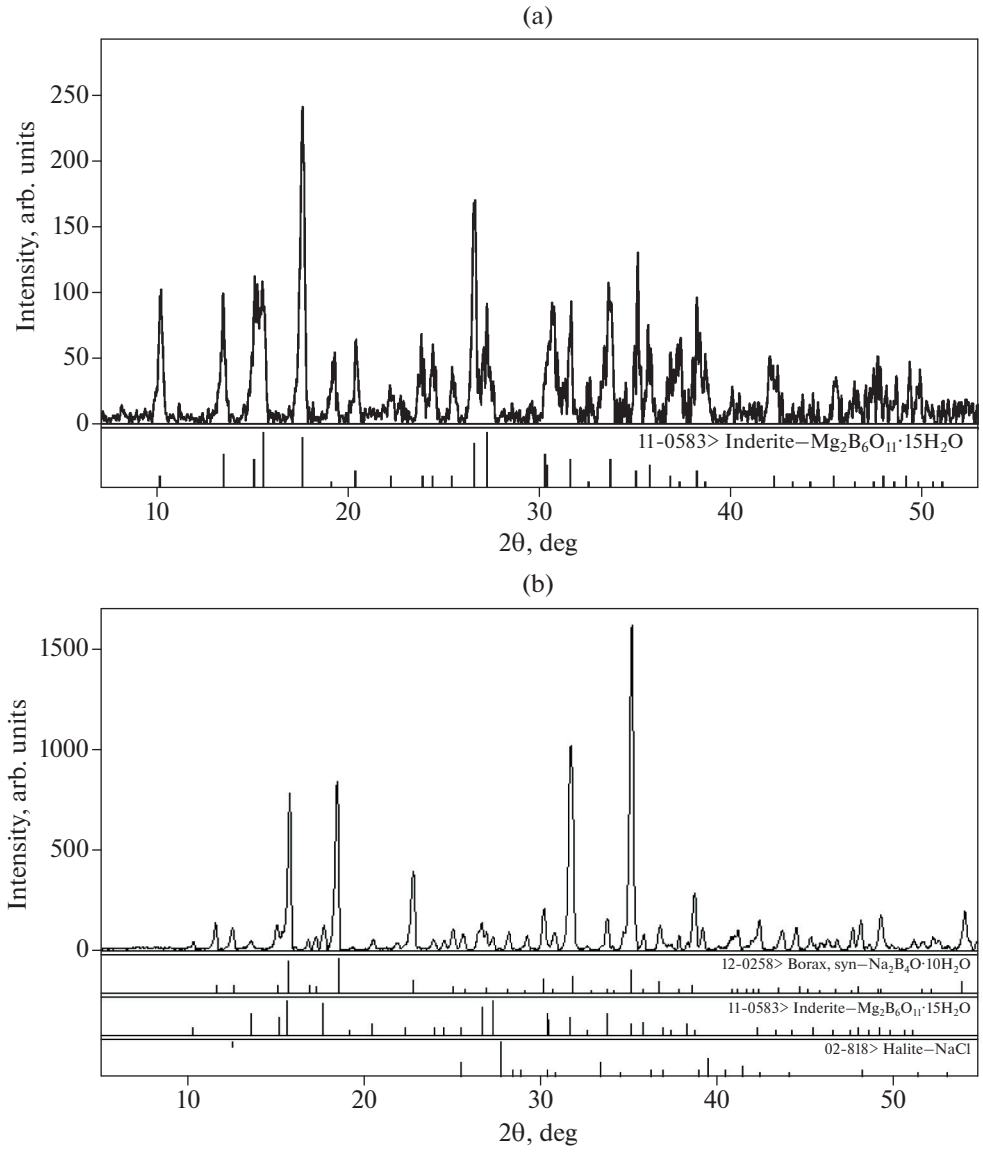

Fig. 3. X-ray diffraction pattern of solid phases: (a) $Mg_2B_6O_{11}·15H_2O$, (b) ($Na_2B_4O_7·10H_2O$ + $Mg_2B_6O_{11}·15H_2O$ + NaCl).

decreased with the increasing concentration of $J(Mg^{2+})$ in the solubility isotherm curve of E_2F_1 and F_1F_2. On the curves of E_2F_1 and F_1F_2, the pH values of the equilibrium liquid phase decreased gradually because of the increase of total Mg^{2+} molality in the solution with dissolving of $MgCl_2$.

CONCLUSIONS

Solid-liquid phase equilibria of the quaternary system Na^+, $Mg^{2+}//Cl^-$, $B_4O_7^{2-}–H_2O$ at 298.15 K were investigated using the isothermal dissolution method. Solubilities and physicochemical properties including density, refractive index and pH value were measured experimentally. Phase diagram of the quaternary system consist of two invariant point and four crystallization regions corresponding to NaCl, $MgCl_2·6H_2O$, $Na_2B_4O_7·10H_2O$ and $Mg_2B_6O_{11}·15H_2O$, respectively. The size of crystallization areas of salt is in the order $Mg_2B_6O_{11}·15H_2O$ > NaCl > $Na_2B_4O_7·10H_2O$ > $MgCl_2·6H_2O$. Hungchaoite ($MgB_4O_7·9H_2O$), an incongruently dissolved solid, represents a metastable phase, which easily convert to $Mg_2B_6O_{11}·15H_2O$. The solution density and refractive index in the quaternary system changed regularly with increasing of $J(Mg^{2+})$ concentration in the solution. This phase diagram can be used to guide the separating process of magnesium and boron salts from the salt lake brine.

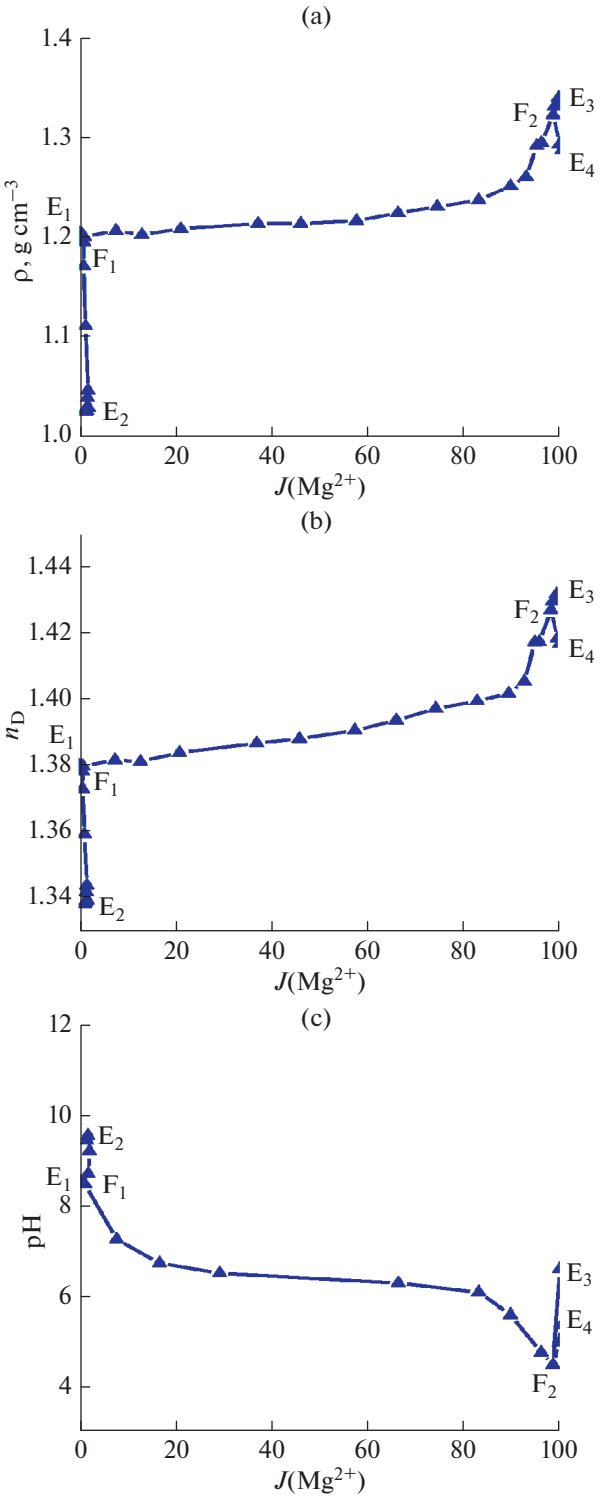

Fig. 4. Diagram of solution physicochemical properties of the quaternary system (Na^+, Mg^{2+}//Cl^-, $B_4O_7^{2-}$–H_2O) at 298.15 K: (a) density, (b) refractive index, (c) pH value.

FUNDING

The work was supported by the Program of the National Natural Science Foundation of China (nos. 22078247, U1707602, and U1507109), the Natural Science Foundation of Hebei Province (B2021202058), and the Yangtze Scholars and Innovative Research Team in University of Ministry of Education of China (IRT-17R81).

CONFLICT OF INTEREST

The authors declare that they have no conflicts of interest.

REFERENCES

1. W. S. Whittingham, Chem. Rev. **104**, 4271 (2004). https://doi.org/10.1021/cr020731c
2. Y. Liu, X. Liu, S. Liu, et al., Angew. Chem. Int. Edit. **59**, 7793 (2020). https://doi.org/10.1002/anie.202001042
3. Z. Y. Guo, Z. Y. Ji, Q.B. Chen, et al., J. Cleaner Prod. **193**, 338 (2018). https://doi.org/10.1016/j.jclepro.2018.05.077
4. A. H. Hamzaoui, A. M'Nif, H. Hammi, et al., Desalination **158**, 221 (2003). https://doi.org/10.1016/S0011-9164(03)00455-7
5. X. Y. Zheng, M. G. Zhang, C. Xu, and B. X. Li, *Salt Lakes of China* (Chinese Science Press, Beijing, 2002).
6. X. Y. Zhao, L. Y. An, and X. Q. Tan, Ind. Miner. Process **5**, 16 (2012). https://doi.org/10.16283/j.cnki.hgkwyjg.2012.05.002
7. H. W. Ge, M. Wang, Y. Yao, et al., J. Chem. Eng. Data **65**, 26 (2019). https://doi.org/10.1021/acs.jced.9b00663
8. Y. Z. J, S. Y. Gao, S. P. Xia, and J. Li, Spec. Acta A **56**, 1291 (2000). https://doi.org/10.1016/S1386-1425(99)00227-9
9. S. Q. Wang, D. Zhao, Y. Song, et al., Russ. J. Phys. Chem. A **92**, 2601 (2018). https://doi.org/10.1134/S0036024418130289
10. S. Q. Wang, X. M. Du, Y. Jing, et al., J. Chem. Eng. Data **62**, 253 (2017). https://doi.org/10.1021/ acs.jced.6b00626
11. H. W. Ge, H. Yang, and M. Wang, J. Chem. Eng. Data **65**, 628 (2020). https://doi.org/10.1021/ acs.jced.9b00852
12. X. P. Zhao, X. P. Zhang, and S. H. Sang, Russ. J. Phys. Chem. A **91**, 1932 (2017). https://doi.org/10.1134/ s0036024417100417
13. D. C. Li, J. S. Yuan, and S. Q. Wang, Russ. J. Phys. Chem. A **88**, 42 (2014). https://doi.org/10.1134/ S0036024414010300
14. T. L. Deng, S. Q. Wang and B. Sun, J. Chem. Eng. Data **53**, 411(2008). https://doi.org/10.1021/je700472p
15. L. Yang, X. F. He, Y. Y. Gao, et al., J. Chem. Eng. Data **63**, 1206 (2018). https://doi.org/10.1021/ acs.jced.7b00800
16. S. Q. Wang, X. M. Du, Y. Jing, et al., Russ. J. Phys. Chem. A, **91**, 2503 (2017). https://doi.org/10.1021/ acs.jced.6b00626

17. S. Q. Wang, Y. Song, X. M. Du, et al., Russ. J. Inorg. Chem. **63**, 116 (2018). https://doi.org/10.1134/ S0036023618010175
18. X. P. Zhao, X. P. Zhang, Y. Y. Yang, et al., J. Chem. Eng. Data **62**, 1377 (2017). https://doi.org/10.1021/acs.jced.6b00926
19. S. H. Song and J. Peng, Chin. J. Chem. **28**, 755 (2010). https://doi.org/10.1134/s0036023620030195
20. S. Tursunbadalov, Russ. J. Inorg. Chem. **65**, 412 (2020). https://doi.org/10.1134/S0036023620030195
21. X. D. Yu, Y. Zeng, S. S. Guo, et al., J. Chem. Eng. Data **61**, 1246 (2016). https://doi.org/10.1021/ acs.jced.5b00888
22. Y. Jing, Sea-Lake Salt Chem. Ind. **2**, 24 (1999). https://doi.org/10.16570/j.cnki.issn1673-6850.2000.02.009
23. F. Yuan, J. Jiang, S. Q. Wang, et al., J. Mol. Liq. **337**, 116334 (2021). https://doi.org/10.1016/j.molliq.2021.116334
24. D. C. Li, R. Fan, S. N. Yang, et al., Chem. Res. Chin. Univ. **34**, 803 (2018). https://doi.org/10.1007/s40242-018-7395-8